ACTA MONTANA IRSM AS CR (1996)
Series A, No. 10 (102), 179–192

FOCAL ZONES OF ROCKBURSTS WITHIN THE SHAFT PILLAR OF MINE KLADNO – 2

JIŘÍ BUBEN, MILOŠ VENCOVSKÝ and ROBERT BROŽ

Institute of Rock Structure and Mechanics of Academy of Sciences of the Czech Republic
V Holešovičkách 41, 182 09 Prague, Czech Republic

ABSTRACT. It is known that rockburst occurrence in the deep coal mine Kladno sometimes satisfies the so-called time predictable random process. But this model of activity of individual focal zones is not applicable generally. One of reasons could be so far little known dependencies on site– and time–variations of mining activity and on geological and tectonic structure of surrounding rockmass. In order to analyze these dependencies, this paper describes new, computer based methods of delimitation of active rockbursts zones. The time– and site–variations of these zones are examined in the future.

KEYWORDS: rockburst, location, prediction, focal zone, migration, rockmassif, fault, seismoacoustics, local seismic array

1. INTRODUCTION

Liquidation of mine Kladno – 2 shaft pillar is going on since the year 1993 by driving of new mine galleries and also by coal mining in several separate coalfaces. Rockburst phenomena with epicentre in this shaft pillar are registered by the mine seismic net [Brož, Buben 1995; Buben, Brož 1996]. In 1995 were registered and located altogether 2289 rockburst phenomena, which magnitude was sufficient for their detection and localization for given noise and instrument conditions. For brevity, from now, we will call these phenomena rockbursts, or rockburst.

Mining in the pillar in the 1995 was carried out at three various locations. Localized rockbursts were assigned from the beginning to these mine locations as to the epicentre zones. To these zones, marked 1, 2, and 3, characteristics of epicentre distribution in time and seismic energy (amplitudes of records from local seismic station Vinařice) were also related. These characteristics then were correlated with galleries advancing and with coal extraction in each coalfaces, which were determining so–called epicentre zones [Brož, Buben 1995].

In this paper, focal zones inside the shaft pillar are newly determined, with regard to distribution of density of both rockbursts foci and released seismic energy. This new determination is much less schematic than the current one, therefore it can be more reliable starting point for consequent research of possibilities of prognosis and prediction of dangerous major rockbursts. This prognosis is based in research

of process of fragile fracturing of surrounding rock massif, leading to the creation of magistral fragile instabilities (rockburst phenomena in mines).

2. SEISMICITY OF FOCAL ZONES

The rockburst activity of original, schematically delimitated zones no. 1, 2 and 3 is characterized by following 2 graphs:

- cumulative daily frequency of phenomena (Fig. 1)
- cumulative daily amplitude of vertical displacement component, registered by photogalvanometric seismograph Vinařice, shown on Fig. 2

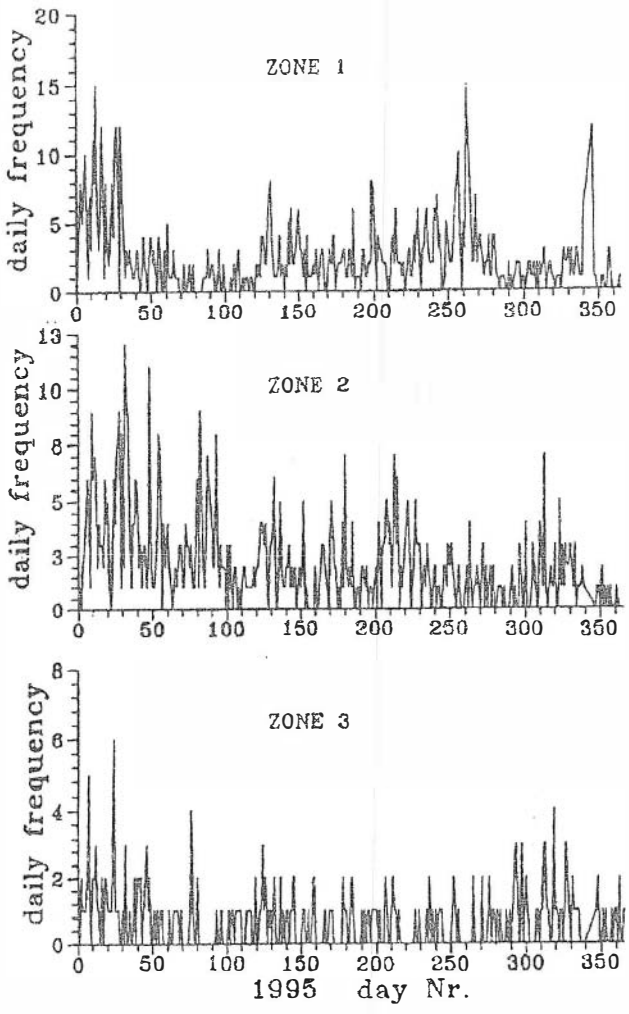

FIG. 1. Daily number of rockbursts in sectors no. 1, 2 and 3

Comparison of these graphs shows that both rockburst activity characteristics of individual zones change in time, but these changes are in no significant mutual correlation. Thus, the course of process leading to origination of rockbursts is not

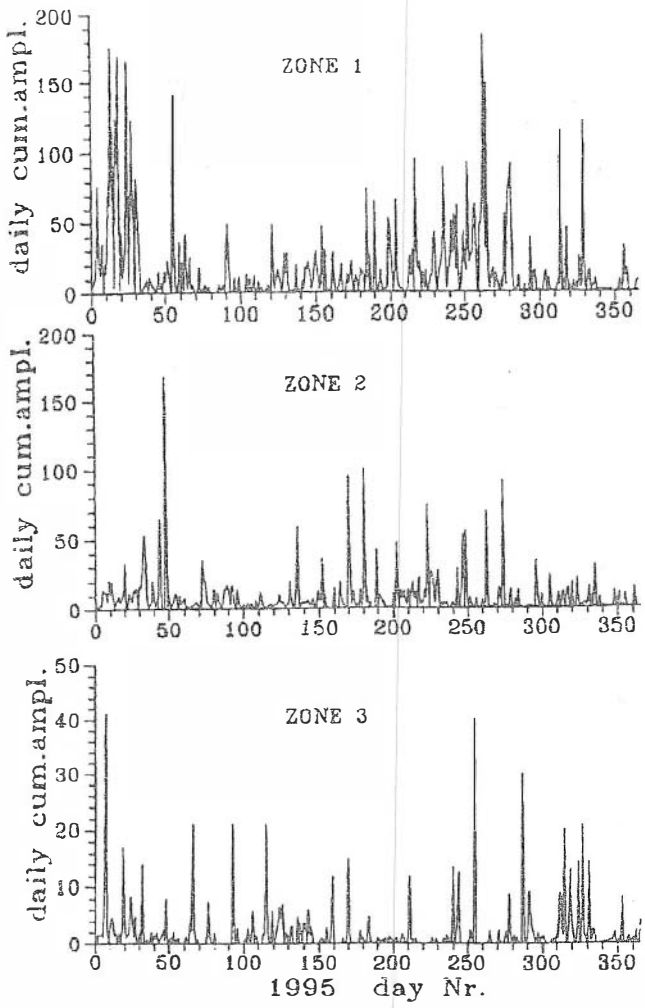

FIG. 2. Daily cumulative amplitudes of rockbursts with foci within sectors no.1, 2 and 3 recorded by seismograph Vinařice

identical in all considered zones. Regional outside forces with significant influence, which is identical in all zones, have therefore negligible magnitude.

Changes of rockburst activity in the zone No.1 are (Fig. 3) characterized by two summary curves:

- daily cumulative maximal amplitude of displacement S_a
- daily frequency of rockbursts S_n

The course of these curves in time is very similar. It is a consequence of a fact that the time changes of rockburst activity can be described by only one of both functions. Recording of number of rockbursts without regard to their magnitude is nonetheless technically much simpler. Therefore, for the routine monitoring, the function S_n is more suitable.

The most studied method of prediction of strong rockbursts is based on evaluat-

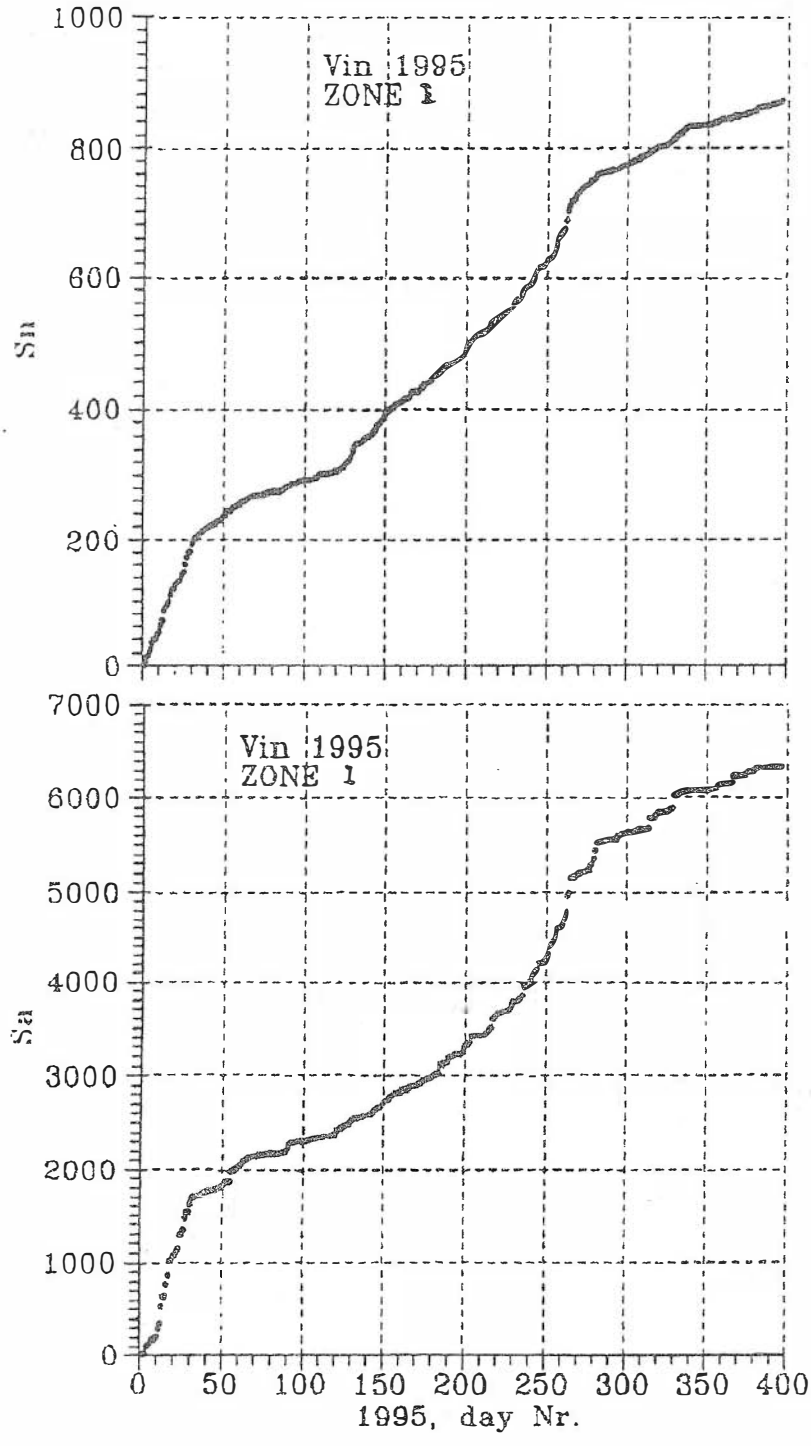

FIG. 3. Cumulative curves of daily number S_n and daily amplitudes S_a of rockbursts in sector no. 1

ing of deviation of velocity of seismic energy release (characterized by the derivative dS_a/dt, resp. dS_n/dt. The usability of this prediction method can be determined using the graph S_a on Fig. 3. Before the occurrence of strong rockburst in the 55th day of the year (24.2.1995), the decrease of slope of curve S_a appears, starting from the day No.30. This phenomenon, though, is not a sufficiently reliable predictor. The anomalous decrease of seismic power (i.e. the decrease of velocity of seismic energy release) did not occur, for example, before the two strong rockbursts in days No.270 (20.9.1995) and 272 (22.9.1995) for values $S_n = 702$ and $S_n = 717$.

As another promising predictor are considered changes of slope β of the following frequency function

$$\log N(m) = A - \beta \cdot m\,, \tag{1}$$

where m is the magnitude of rockburst.

The value β relates according to the known U_{tsu} formula to the average magnitude $E(m)$ of rockbursts, which occurred in certain time interval (e.g. 24 hours). Changes of average amplitude $E(m)$ can be seen on Fig. 4 graph. The horizontal axis represents values of daily cumulative frequency, the vertical axis shows values of daily cumulative amplitude. The slope of this curve dS_a/dS_n so indicates the value of mean amplitude. Strong rockbursts of Sept.20 and Sept.22 1995 are identifiable on this graph for coordinates $S_n = 702$ and $S_n = 717$. They show as distinct skips of values Sa and are recognizable as gaps on this curve. But the course of this curve also shows that before the occurrence of another strong rockbursts, application of this predictor fails.

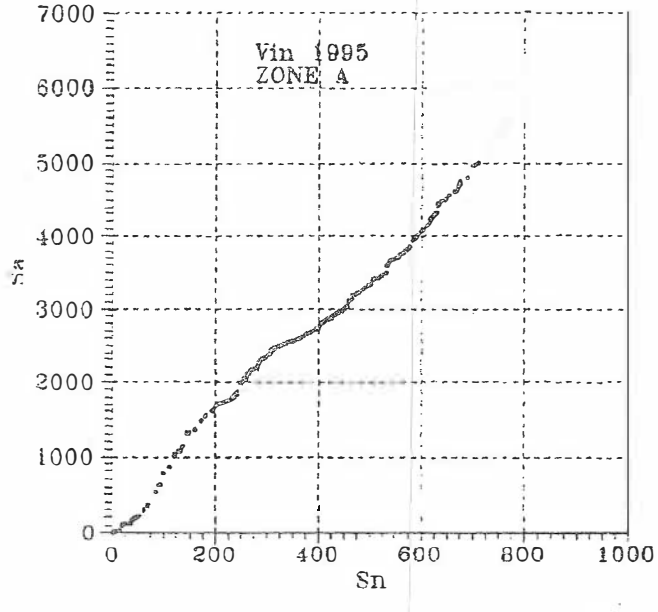

FIG. 4. Changes of mean amplitude daily frequency S_n of rockbursts in sector no. 1

One of possible causes of negative results of testing of statistical predictors of rockbursts can be both present schematic (physically unwarranted) focal zones delimitation, and neglecting the influence of irregular mining works advances in place and also in time, and the impact of geological factors.

3. A New Delimitation of Focal Zones

This delimitation could have been carried out only after resolving of location of many rockburst foci [Ružek 1995]. It is based on determination of density of epicentre rockburst phenomena in elements of square net [Vencovský 1996] with the side of 50 m.

Fig. 5a shows the distribution of density of all rockbursts for the year 1995 as isolines. Fig. 5b show zones A, B and C, delimitated with regard to the density distribution from Fig. 5a. On Fig. 5a, similarly as on Fig. 5b, are marked newly driven galleries (dotted lines) and stopping faces (lined are as) in the year 1955.

Delimitation of zone A was carried out also on the basis of the analysis of seismic energy release velocity, i.e., seismic power of elementary zones. Seismic energy E is defined by

$$\log E = 2 + 1.5 \cdot m\,, \tag{2}$$

where m is local magnitude [Brož, Buben 1995].

The comparison of results of both procedures is shown on Fig. 6. Fig. 6a depicts isolines of relative density of epicentre and Fig. 6b show isolines of seismic power. Both figures are constructed for a square net with double density as compared to frequency analysis from Fig. 5, i.e., for a length of 25 m of elementary square side. Reason for this increase in density was to attain higher resolution capability of the analysis.

Comparing partial Figs. 6, it is obvious that zones delimitated on the basis of epicenter density so as on the basis of seismic power differ only in details one from each other.

4. Changes of Shape and Location of Focal Zones

As was already stated in connection with Fig. 5, zones of epicenter concentration A, B and C were identified from the set of all rockbursts in the 1995. But the subject of research were also time changes of epicenter zones locations and finding possible relation of their migration to advances in mine works.

The distribution of rockbursts epicenter density in individual months is given on Fig. 7. From the study of these figures, it follows that

- zone A is both location–wise and function–wise very conspicuous and stable,
- zone C has similar characteristics, even though some changes in its location already occur
- zone B appears to be very little outstanding

Dependencies of epicenter zones on gallery driving, blasting works and mining itself, though, could not have been examined in sufficiently short, i.e. daily, time intervals. For this correlation analysis,

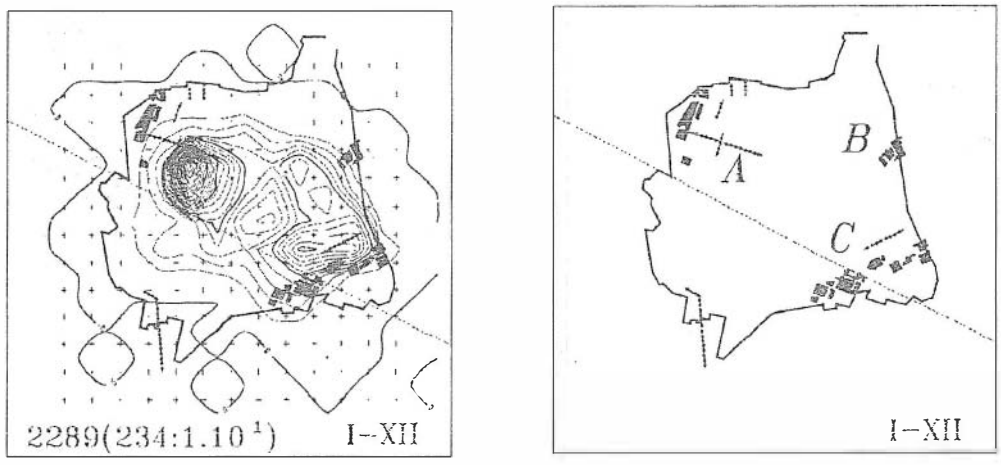

FIG. 5. Density distribution of rockbursts foci and mining activities

FIG. 5a – Density distribution of rockbursts foci registered in the year 1995 (first number of double figure down at left in the bracket is the absolute density in maximum of isoline field, second number is the value of isoline interval. The number in front of the bracket gives the absolute number of all registered rockbursts).

FIG. 5b – Delimitation of foci zones A, B and C and overview of mining activities in the year 1995 (driven galleries as ⟿, tectonic fractures as ——).

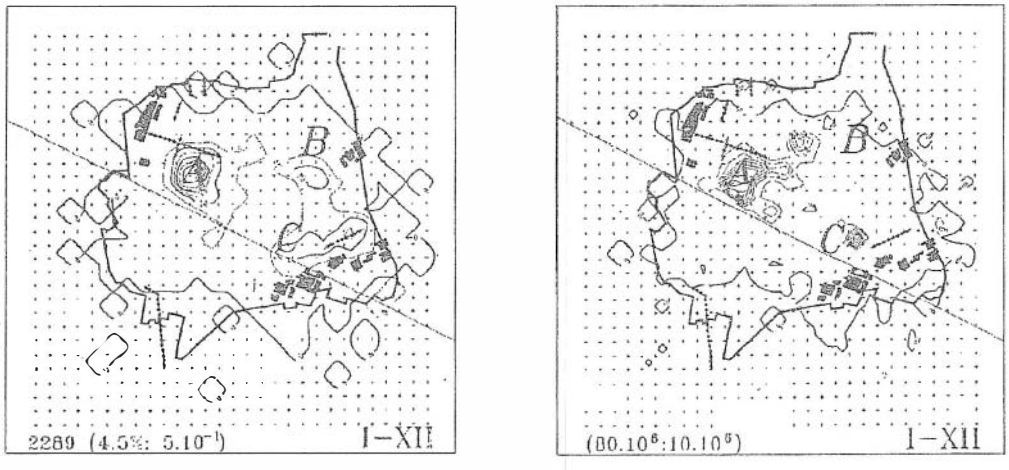

FIG. 6. Alternative delimitation of epicentral zones in the square net with sides of 25 m

FIG. 6a – isolines of relative density

FIG. 6b – isolines of seismic power

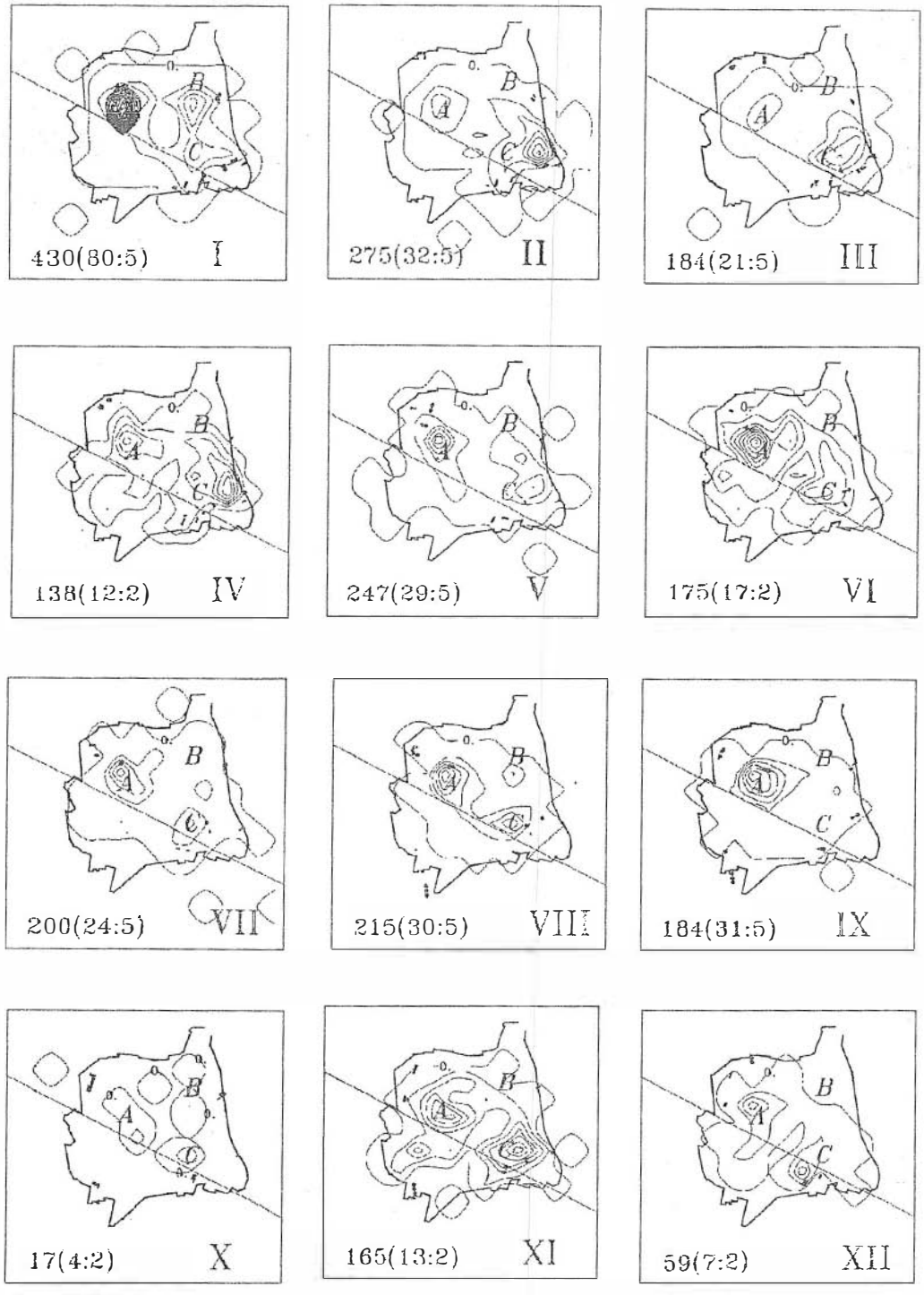

FIG. 7. Density isolines of rockbursts foci for months I to XII in comparison with locations of newly driven galleries and faces, indicated the same as on Fig. 5. Numbers at down left corner have the same meaning as on Fig. 5.

Mining activities, though, do represent, without doubt, a significant triggering mechanism. Its efficiency depends on structural–geological properties of surrounding massif:

(1) petrographical and physical–mechanical characteristics of overlying rock
(2) fracture structures, disturbing rock massif in the pillar,
(3) mutual orientation of mine works and tectonic directions

Petrographical classification of overlying sandstones was carried out using samples taken from following depths:

(1) to 5. floor – depth of 254 m,
(2) to 7. floor – depth of 400 m,
(3) to 10. floor – depth of 510 m.

In the geological profile of pit MAYRAU are registered altogether 41 positions of sandstones and 33 positions of claystones. To research their influence, the pit profile was divided on parts 100 m thick, in which the ratio of total thickness of claystones and sandstones was evaluated. Results are given in following Tab. 1.

TAB. 1.

depth m		thickness ratio
from	to	
	100	1 : 2.6
100	200	1 : 1.1
200	300	1 : 1.4
300	400	1 : 3.7
400	500	1 : 4.3
500	516	1 : 7.0

It is obvious from this table, that conspicuous change of ratio occurs in depths of 300 m and deeper.

It is remarkable that the majority of rockbursts is also clustered in depth of around 300 m. This result was deduced from the analysis of space distribution of rockburst foci density. This analysis was carried out on the basis of determining the number of rockbursts in the space net of elementary cubes with sides of 50 m, filling the overlying space of coal seam. Results of this analysis are shown on Figs. 8a and 8b. The horizontal section 0–0 with the maximum rockbursts concentration corresponds to the depth no other than 300m under the pit bank of mine MAYRAU. Density distribution in vertical sections 1–1 and 2–2 then indicates, that variations in time are not conclusive. The depth distribution of all rockbursts for the year 1995 is indicated on Fig. 8c, from which it follows then, that foci concentrate in the depth H of around $350\,\mathrm{m} \leq H \leq 300\,\mathrm{m}$ under the surface.

This fact also explains low reliability of until now attempts of seismoacoustic prediction of Kladno rockbursts. Seismoacoustic pick–up devices — geophones —

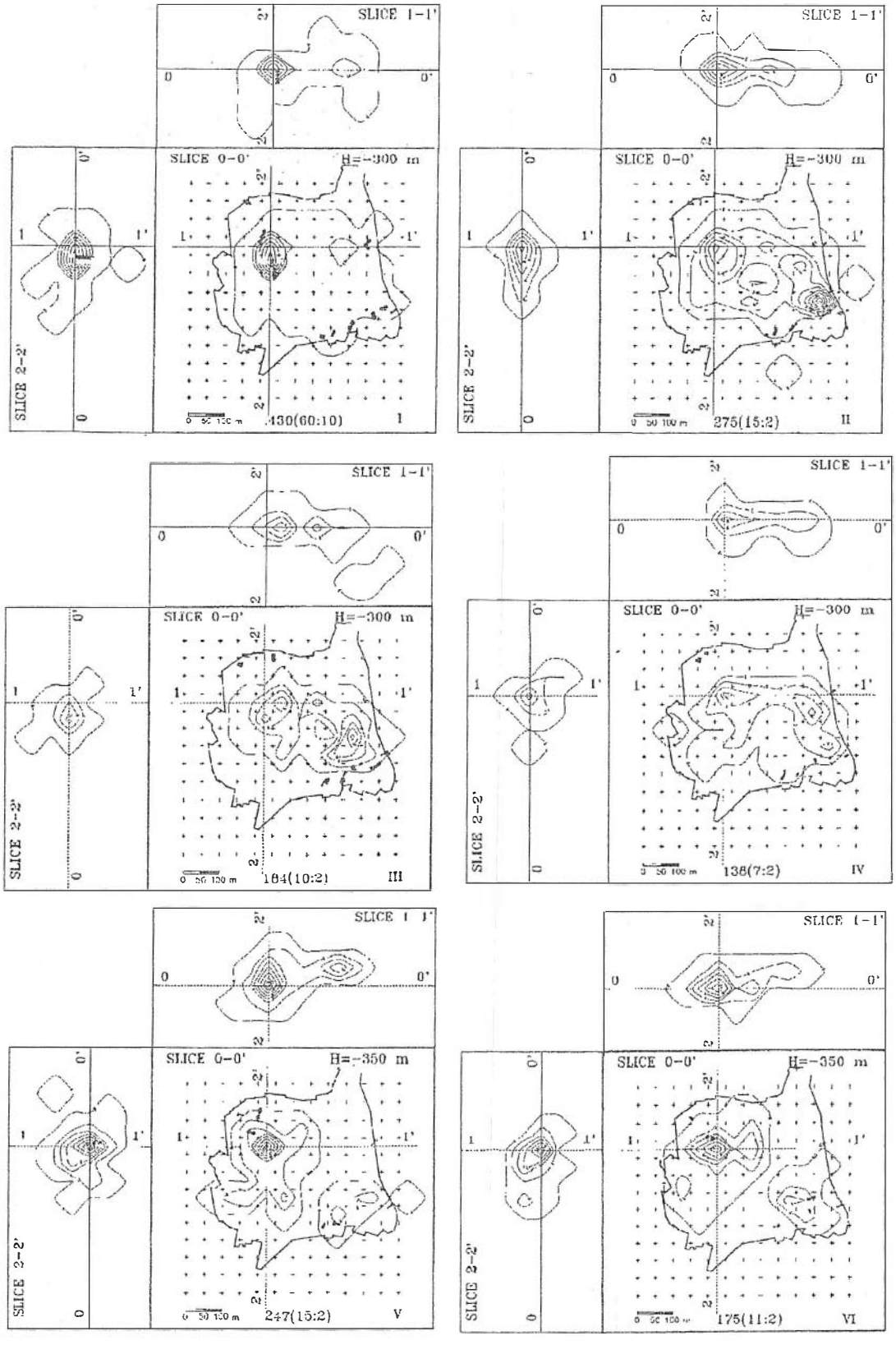
SLICE 1-1'
SLICE 0-0'
H=-300 m
SLICE 2-2'
430(60:10)
I
SLICE 1-1'
SLICE 0-0'
H=-300 m
SLICE 2-2'
275(15:2)
II
SLICE 1-1'
SLICE 0-0'
H=-300 m
SLICE 2-2'
184(10:2)
III
SLICE 1-1'
SLICE 0-0'
H=-300 m
SLICE 2-2'
138(7:2)
IV
SLICE 1-1'
SLICE 0-0'
H=-350 m
SLICE 2-2'
247(15:2)
V
SLICE 1-1'
SLICE 0-0'
H=-350 m
SLICE 2-2'
175(11:2)
VI

FIG. 8a

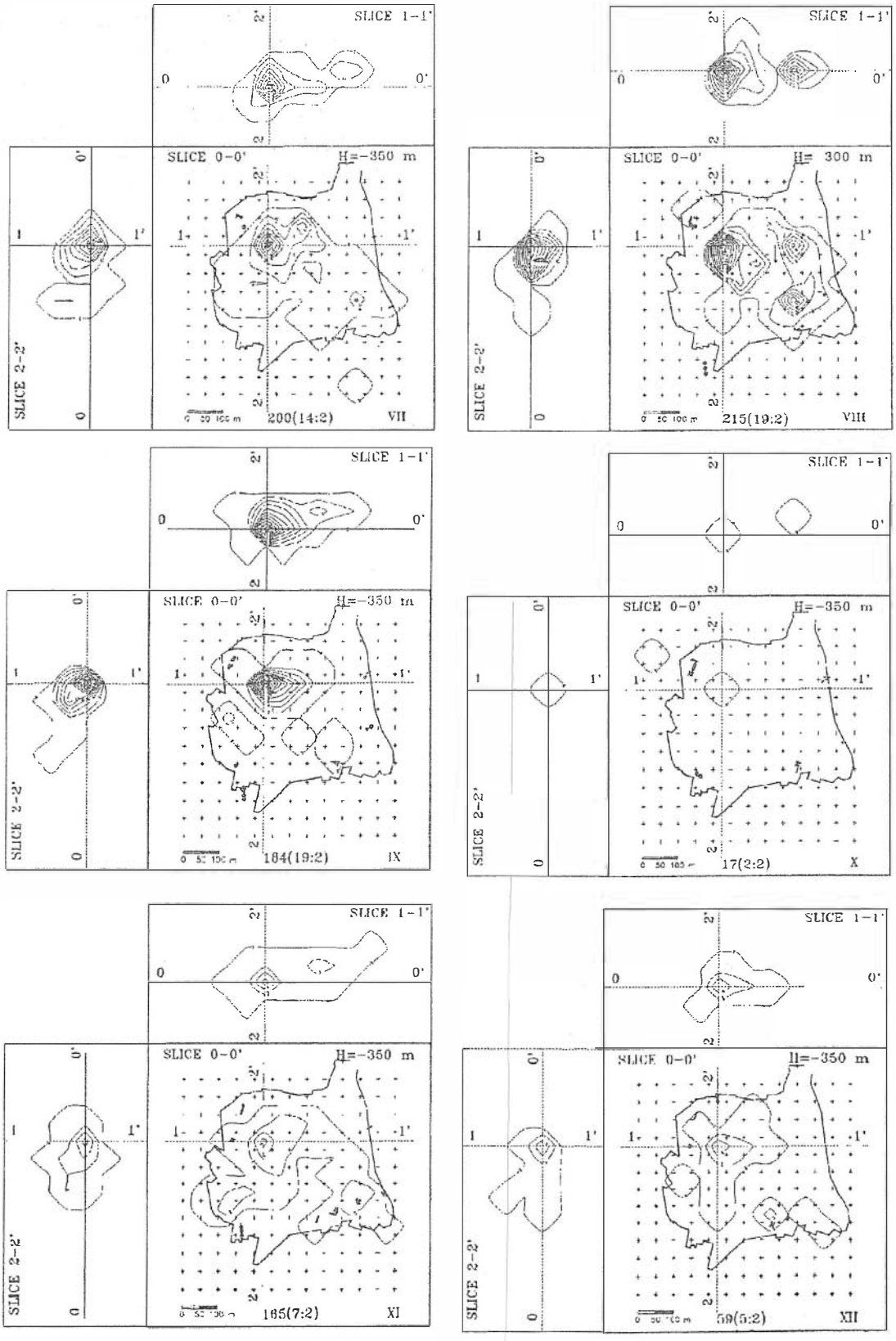
SLICE 1–1'
SLICE 0–0'
H=–350 m
SLICE 2–2'
200(14:2)
VII
SLICE 1–1'
SLICE 0–0'
H= 300 m
SLICE 2–2'
215(19:2)
VIII
SLICE 1–1'
SLICE 0–0'
H=–350 m
SLICE 2–2'
184(19:2)
IX
SLICE 1–1'
SLICE 0–0'
H=–350 m
SLICE 2–2'
17(2:2)
X
SLICE 1–1'
SLICE 0–0'
H=–350 m
SLICE 2–2'
165(7:2)
XI
SLICE 1–1'
SLICE 0–0'
H=–350 m
SLICE 2–2'
59(5:2)
XII

FIG. 8b

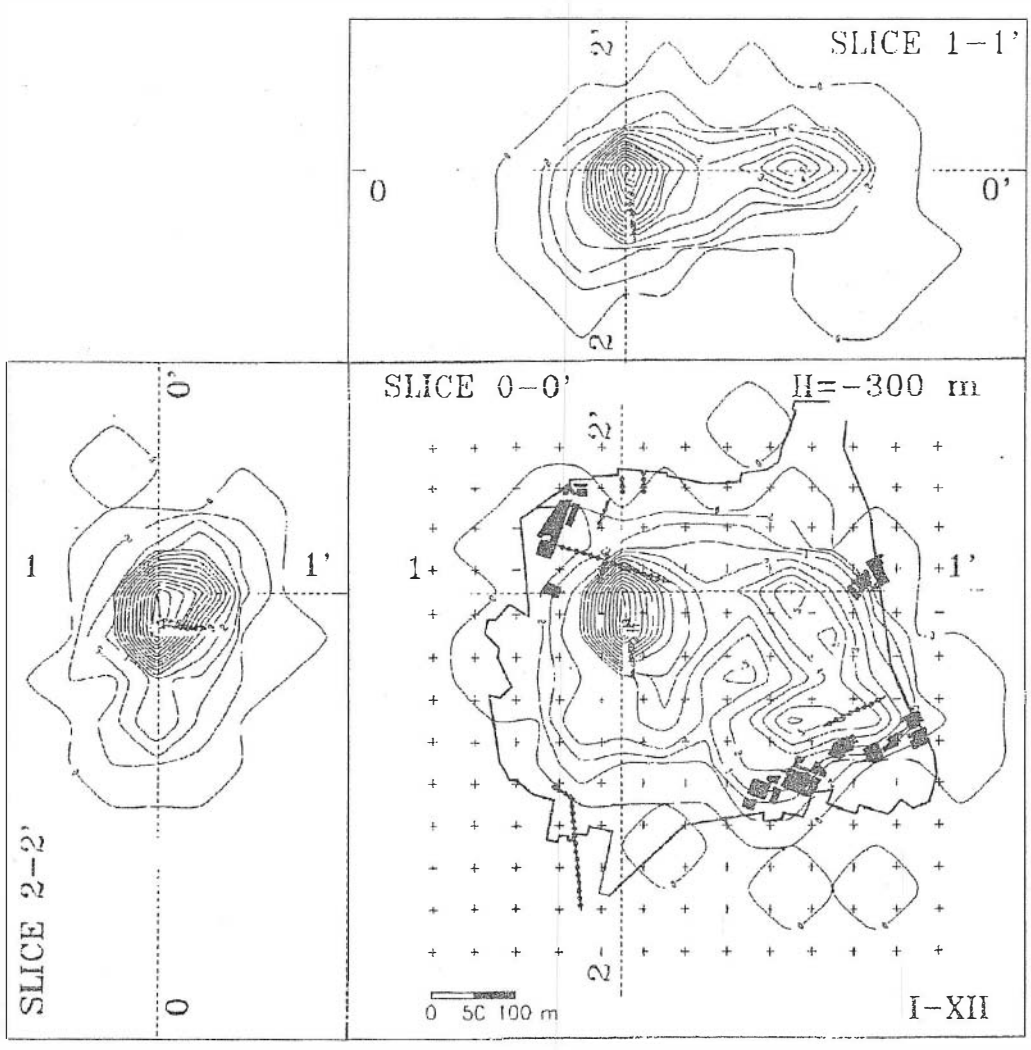

FIG. 8c

FIG. 8 Three–dimensional density distribution of rockbursts foci

FIGS. 8a and 8b – distribution by individual months I to XII. Section 0–0 runs through the horizontal plain in the depth of $H = 300$ m to $H = 350$ m under the surface, newly driven galleries and faces are also indicated. Sections 1–1 and 2–2 are led in the direction of both axis of horizontal coordinates system. Numbers at the bottom have the same meaning as on Fig.5.

FIG. 8c – distribution for the whole year 1995

were, from reasons of simplicity and low mine–technical requirements, until now always installed in small distance from mining galleries, i.e., in distance of about 200 m under the center of foci zones. In these conditions, the satisfying ratio of

useful and perturbation impulses could not have been reached. Geophones were placed nearby disturbing signals sources (all kinds of mining activities), and too far from foci of relatively weak seismoacoustic manifestations of fragile instabilities in rockmassif.

In the shaft pillar, there are two main tectonic faults, which on the 10th floor run in the NW – SE direction, see Figs. 5a,5b. This direction is characteristic also for minor tectonic faults in the pillar.

First from these main faults divides the shaft pillar in half almost diagonally, as indicated by an dashed line on the Fig. 5a,b and also on Fig. 7. In its NW part, it has a NE sense of inclination with the angle of 70°. Similarly, also the height of skip is the biggest in NW part, where it reaches 15 m, and decreases to 7 m at the SE rim of the pillar.

The second main fault cuts the NE border of the pillar, and has in this place a NE sense of inclination, angle of 22° and height of skip 0.5 m. Towards the SE then it changes to the opposite sense of inclination, i.e. NW inclination with the angle of 60°. The skip in this part of fault is 12 m.

The coupling of foci zones on fault structures documents Fig. 7. The main fault NW – SE clearly appears as a dividing line between rockburst and non-rockburst part of the pillar. This is confirmed by the distribution of foci zones A and C. Rockbursts cluster in locations where the angle of inclination is bigger. In the zone A, this angle is 70° and in the zone B it is 60°. Foci zones adhere to faults and adjust to them with their shape. The height of skip on the faults reaches maximum value within the foci zones, that is 15 m in zone A, and 12 m in zone C.

On Fig. 7 it is also possible to follow the clear relation between the galleries driving and rockburst activity: in the active zone C, no galleries were driven in months no. 2, 3, 4, 5 and 11. As a rule it holds, that rockbursts foci occur nearby galleries being driven. For the zone A, this is most clearly visible in month 1. For both zones A and C, the impact of galleries driving can be identified also for months 2, 3, 4, 5, 11 and 12. Driven galleries do not initiate rockbursts foci, when they run close to old man, which is documented by partial pictures for months 3, 9, 10, 11 and 12. Also, the mining nearby old man did not induce rockbursts in months 2, 3, 4, 9, 10 and 12.

The dependence between places of mining activity itself and position of foci zones was not reliably to be found. Analyses of all partial pictures from Fig. 7 lead only to little provable correlations. To deeper analyze these relations, prognoses of undermining impacts were carried out. All mined–out areas for the year 1995 for the horizon approx. 300 m under the surface — i.e. for depth where rockbursts accumulate the most — were considered. A special signification in this direction is being ascribed to prognoses of horizontal displacement changes, from which areas of maximum tensions and compressions can be identified, and also to prognoses of sinking changes, which can thereafter delimitate areas, where horizontal layers of rock massif are most bend–stressed [Vencovský 1995]. Isolines of prognosed horizontal and vertical deformations are shown on Fig. 9. A locational confrontation of areas with maximum horizontal and vertical deformations with foci zones from Fig. 8g leads to the suggestion that outside the borders of shaft pillar, rockburst

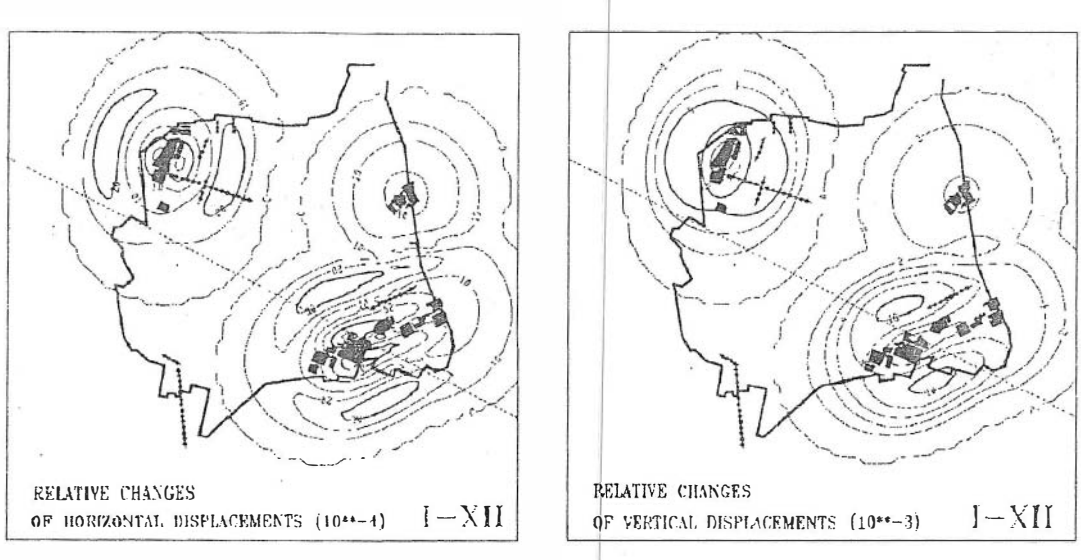

FIG. 9. Results of theoretical calculation (prognosis) of deformation isolines induced by excavations in the year 1995

FIG.9a – isolines of horizontal deformation component

FIG.9b – isolines of vertical deformation component

practically do not occur, even though the prognosed maximum deformation zones involve also the outside of the pillar. This found displacement of active zones in direction from the borders towards the center of the shaft pillar, and obvious asymmetry of rockbursts occurrence with the mining activity are at present the subject of more detailed analyses, which results will be published in the future. Subject of further study is also testing of predictors with the use of filtered data from newly delimitated focal zones.

Acknowledgement: This paper was particularly funded by the Grant Agency of the Czech Republic, registration number of the project 105/96/1065.

REFERENCES

Brož R., Buben J. (1995), *Interpretation of Rockbursts Recorded by the Local Seismic Station Kladno – Vinařice during the Year 1993*, Acta Montana **A7** (96), 21–51.

Buben J., Brož R. (1996), *Interpretation of Rockbursts Recorded by the Local Seismic Station Kladno – Vinařice during the Year 1994*, Acta Montana **A9** (100), 139–157.

Vencovský M. (1995), *Prediction of Surface Motion during the Exploitation of the Pillar in the Coal Mine Mayrau*, Acta Montana **A7** (96), 83–113.

Vencovský M. (1996), *Density of Flat Field Points*, Geodetic and Geographic Review, in print. (in Czech)